学位論文
Doctoral Thesis

Usefulness of diffusion-weighted magnetic resonance imaging and (18)F-Fluorodeoxyglucose PET-CT in the diagnosis and predicting aggressiveness of non-small cell lung cancer

（小型非小細胞肺癌の診断と悪性度指標としての拡散強調画像および FDG-PET の有用性）

大場　康臣

Yasuomi　Ohba

熊本大学大学院医学教育部博士課程臨床医科学専攻呼吸器外科学

指導教員

鈴木　実　　教授

熊本大学大学院医学教育部博士課程医学専攻呼吸器外科学

野守　裕明　前教授

熊本大学大学院医学教育部博士課程医学専攻呼吸器外科学

2011年3月

学　位　論　文

Doctoral Thesis

論文題名　：　Usefulness of diffusion-weighted magnetic resonance imaging and (18)F-Fluorodeoxyglucose PET-CT in the diagnosis and predicting aggressiveness of non-small cell lung cancer

（小型非小細胞肺癌の診断と悪性度指標としての拡散強調画像および FDG-PET の有用性）

著 者 名　：　大場　康臣
Yasuomi　Ohba

指導教員名　：　鈴木　実　教授
野守　裕明　前教授

熊本大学大学院医学教育部博士課程臨床医科学専攻呼吸器外科学

審査委員名　：　放射線診断学担当教授　山下　康行
心臓血管外科学担当教授　川筋　道雄
呼吸器病態学担当教授　興梠　博次
乳腺・内分泌外科学担当教授　岩瀬　弘敬

２０１１年３月

Table of Contents

Abstract

Background and Purpose

Until recently, the usefulness of diffusion-weighted magnetic resonance imaging has been reported in the imaging of malignant tumors. And it was reported that diffusion-weighted magnetic resonance imaging had similar sensitivity and specificity as compared to fluorodeoxyglucose F 18 positron emission tomography for distinguishing between malignant and benign pulmonary nodules. This retrospective analysis examined whether diffusion-weighted magnetic resonance imaging might be as useful as positron emission tomography with fludeoxyglucose F 18 for (1) discriminating between non–small cell lung cancer and benign pulmonary nodules and (2) predicting aggressiveness of non–small cell lung cancer to successfully select patients for limited resection .

Methods

Diffusion-weighted magnetic resonance imaging and fluorodeoxyglucose F 18 positron emission tomography were performed before surgery in 110 patients with 124 pulmonary nodules smaller than 3 cm, including 96 non–small cell lung cancers and 28 benign nodules. Diffusion of water molecules in magnetic resonance imaging was measured by minimum value of apparent diffusion coefficient. The criterion standard was the result of histologic diagnosis or follow-up examination. Sensitivity and specificity for differentiating between cancers and benign nodules were compared between diffusion-weighted imaging and positron emission tomography. Apparent diffusion coefficient in diffusion-weighted imaging and fludeoxyglucose F 18 uptake in positron emission tomography were examined with respect to pathologic tumor stage; lymphatic, vascular and pleural involvements; histologic differentiation; and proliferative activity as determined by immunostaining with Ki-67.

Results

There were no significant differences between diffusion-weighted magnetic resonance imaging and fluorodeoxyglucose F 18 positron emission tomography in sensitivity or specificity for non–small cell lung cancer. Whereas positron emission tomography showed significant differences in fludeoxyglucose F 18 uptake between pathologic stages IA versus IB or more advanced stages; between tumors with and without lymphatic, vascular, or pleural involvement; between Ki-67 staining scores; and between well-differentiated and moderately or poorly differentiated adenocarcinomas ($P<.01–0.001$), no significant differences in apparent diffusion coefficient values in were observed.

Conclusions

Diffusion-weighted magnetic resonance imaging is equivalent to fluorodeoxyglucose F 18 positron emission tomography in distinguishing non–small cell lung cancer from benign pulmonary nodules but is not as useful for predicting aggressiveness of non–small cell lung cancer to successfully select patients for limited resection.

Japanese abstract

背景:近年、拡散強調 MRI 画像（DWI）の悪性腫瘍の画像診断における有用性が報告されてきている。肺領域では、肺悪性腫瘍と良性結節の鑑別においてDWI は fluorodeoxyglucose F 18 positron emission tomography （FDG-PET）と同等に有用であるとの報告がある。今回、我々は非小細胞肺癌の診断ならびに悪性度指標としての DWI の有用性について、FDG-PET と比較検討を行った。

対象と方法:2006 年 2 月より 08 年 2 月までの術前に FDG-PET および DWI を行った長径 1～3cm の肺結節のうち、pure GGO 症例を除外した 110 例、124 結節を対象とした。このうち、非小細胞肺癌 96 例、良性結節 28 例であった。ROC カーブを用いて SUV-CR-lung（結節と対側肺の SUVmax の比）および ADC-min（結節の拡散係数の最低値）の cut off 値を決定し、SUV-CR≧0.31、ADC-min< $1.2x10^{-3}mm^2/s$ を陽性とした。また、腫瘍の悪性度指標として①病理病期、②腫瘍内脈管浸潤・胸膜浸潤の有無、③組織学的分化度、④Ki-67 staining scores を用い、これらと SUV-CR 値、ADC-min 値との関連を検討した。

結果:DWI と PET の非小細胞肺癌診断の感度はそれぞれ 0.73、0.72、特異度は 0.96、0.82 でいずれも有意差は認めなかった。病理病期 IA 期 75 例と IB 期以上 21 例の SUV-CR の平均値はそれぞれ 0.45±0.27vs0.74±0.16 と、IB 期以上の進行肺癌で有意に高値であった（p<0.001）が、ADC-min ではそれぞれ 1.00±0.34 vs0.83±0.20 と有意差は認めなかった（p=0.08）。腫瘍内脈管浸潤・胸膜浸潤や組織学的分化度、Ki-67 staining scores において SUV-CR 値とはそれぞれ有意な相関を認めた（p<0.01–0.001）が、ADC-min 値とはいずれも相関を示さなかった。

結語:DWI は小型非小細胞肺癌と良性結節との鑑別においては FDG-PET と同等に有用であると考えられるが、非小細胞肺癌の病理病期、腫瘍内脈管浸潤・胸膜浸潤や肺腺癌における組織学的分化度や Ki-67 staining scores との相関は認めなかった。3cm 以下の小型非小細胞肺癌の悪性度予測においては DWI の有用性は低いのではないかと考えられ、縮小手術の適応評価としては FDG-PET が適していることが示唆された。

Publication list

① 関連論文

1. Is diffusion-weighted magnetic resonance imaging superior to positron emission tomography with fluorodeoxyglucose in imaging non-small cell lung cancer?

   Ohba Y, Nomori H, Mori T, Ikeda K, Shibata H, Kobayashi H, Shiraishi S, Katahira K.

   J Thorac Cardiovasc Surg. 2009 Aug;138(2):439-445.

② その他の論文

2. Evaluation of semiquantitative assessments of fluorodeoxyglucose uptake on positron emission tomography scans for the diagnosis of pulmonary malignancies 1 to 3 cm in size.

   Ohba Y, Nomori H, Shibata H, Kobayashi H, Mori T, Shiraishi S, Nakashima R.

   Ann Thorac Surg. 2009 Mar;87(3):886-91.

3. Required area of lymph node sampling during segmentectomy for clinical stage IA non-small cell lung cancer.

   Nomori H, Ohba Y, Shibata H, Shiraishi K, Mori T, Shiraishi S.

   J Thorac Cardiovasc Surg. 2010 Jan;139(1):38-42

4. Positron emission tomography in lung cancer.

   Nomori H, Ohba Y, Yoshimoto K, Shibata H, Shiraishi K, Mori T.

   Gen Thorac Cardiovasc Surg. 2009 Apr;57(4):184-91.

5. Difference of sentinel lymph node identification between tin colloid and phytate in patients with non-small cell lung cancer.

Nomori H, Ohba Y, Yoshimoto K, Shibata H, Mori T, Shiraishi S, Kawanaka K, Kobayashi T.

Ann Thorac Surg. 2009 Mar;87(3):906-10.

Acknowledgements

These series of investigation were performed from 2007 to 2010, in the Department of Thoracic surgery, Graduate School of Medical Sciences, Kumamoto University.

I wish to extend my warmest thanks to Professor Makoto Suzuki and former Professor Hiroaki Nomori, the department of Thoracic surgery, Graduate School of Medical Sciences, Kumamoto University. They generously gave me advice and suggestions.

I am grateful to all staffs in the department of Thoracic surgery, Graduate School of Medical Sciences, Kumamoto University. They provided me with their valuable time and gave me much advice.

Finally, I would like to thank my family for their support, encouragement and unshakable faith in my abilities during the course of my studies.

Abbreviations and Acronyms

ADC = apparent diffusion coefficient

CT = computed tomography

DWI = diffusion-weighted magnetic resonance imaging

FDG = fludeoxyglucose F 18

FDG-PET = positron emission tomography with fludeoxyglucose F 18

FN = false-negative result

FOV = field of view

FP = false-positive result

GGO= ground-glass opacity

MR = magnetic resonance

NSCLC= non-small cell lung cancer

PET = positron emission tomography

ROI = region of interest

ROC= receiver operating characteristic

SUV = standard uptake value

SUVCR = contrast ratio of standard uptake value

SUVmax = maximum standard uptake value

TE = echo time

TN = true-negative result

TP = true-positive result

TR = repetition time

VATS= video-assisted thoracic surgery

Background and Purpose

The detection of small peripheral non-small cell lung cancer (NSCLC) has increased with the advent of more sophisticated imaging modalities, such as high resolution computed tomography (CT) [1]. Furthermore, surgery using video-assisted thoracic surgery (VATS) has contributed to preserved postoperative respiratory function and improvement in the postoperative course, particularly in high risk patients [2,3].

In addition, VATS can be well indicated for limited operations such as wedge resection and segmentectomy [4–6]. Trials of limited operations for small peripheral NSCLC, in particular for high risk patients, have demonstrated the eligibility of such patients for limited operations [7,8]. To successfully select patients for limited resection, patients with good prognosis preoperatively should be chosen.

However because there have been no sufficient data to support the efficacy of limited operation for clinical stage IA NSCLC, it is not the standard of care yet. One of the reasons is that clinical stage is an inadequate parameter by which to judge the suitability of such an alternative to the conventional lobectomy, since a substantial proportion of small peripheral NSCLC patients are at a more advanced stage than clinically defined. For instance, 15–30% of lymph node metastases in peripheral NSCLC are less than 3 cm in diameter [9–11].

Even for patients with pathologic T1 N0 M0 NSCLCs, tumor involvement of intratumoral vessels or the pleura can also cause local recurrence after limited

resection because of the spread of tumor cells into lymphatic vessels outside the primary tumor. To predict which T1 N0 M0 lung adenocarcinomas are curable with limited resection from CT findings, several reports have evaluated the importance of ground-glass opacity (GGO) within tumors, usually indicating bronchioloalveolar carcinoma– like spread because adenocarcinomas with GGO appearance are more frequently N0 stage and have less tumor involvement of intratumoral vessels or pleura than those with a solid appearance (12,13). The criteria of defining GGO appearance on CT scans are subjective, however, potentially leading to erroneous selection of limited surgical intervention.

Recent advances in magnetic resonance (MR) gradient technology have led to the introduction of diffusion-weighted MR imaging (DWI), which provides excellent tissue contrast based on differences in the diffusion of water molecules among tissues and is entirely different from ordinary T1- and T2-weighted MR images. Because the diffusion of water molecules is disturbed by intracellular organelles and macromolecules, any architectural changes in the proportion of extracellular to intracellular water molecules alters the signal intensity on DWI, i.e., the values of the apparent diffusion coefficient (ADC) [14,15]. As malignant tumors are characterized by increased cellularity, larger nuclei with more abundant macromolecular proteins, larger nuclear cytoplasmic (N/C) ratio, and less extracellular space as compared with normal tissues, the diffusion of water molecules in malignant tumors is restricted, resulting in a decrease of the ADC values, which allows imaging of malignant tumors by DWI [16,17]. Until recently, the usefulness of DWI has been reported in the

imaging of brain tumors [18], breast tumors [19], musculoskeletal tumors [20], prostate cancer [21], rectal cancer [22] and lung cancer [23].

On the other hand, positron emission tomography (PET) using ^{18}F-fluorodeoxygludose (FDG) has been found to be extremely useful for discriminating between malignant and benign pulmonary nodules. While several authors have compared the images between DWI and PET in a small number of tumors [24,25], there have been few reports of comparison of the sensitivity and specificity of DWI and FDG-PET for diagnosing malignancy. Recently, we showed that DWI had similar sensitivity and a slightly higher specificity as compared to FDG-PET for distinguishing between malignant and benign pulmonary nodules [26]. On the other hand, Ohno et al. reported that whole-body MR imaging with DWI had similar accuracy to FDG-PET for M-staging in NSCLC patients [27]. However, FDG-PET has been reported to be also able to assess tumor aggressiveness, including the tumor stage and intratumoral invasiveness, and the prognosis of the patients [28-31]. Therefore, while comparing the relative merits of DWI and FDG-PET in cases of NSCLC, the usefulness of the examinations for both the diagnosis and evaluation of tumor aggressiveness should be compared.

In the present study, we conducted a retrospective analysis of the subject data with the following 2 objectives: (1) to examine the usefulness of DWI in the differential diagnosis of pulmonary nodules by comparing the sensitivity and specificity of DWI and FDG-PET for discriminating between NSCLC and benign pulmonary nodules; and (2) to compare the usefulness of DWI and PET to predict the

aggressiveness of NSCLC to successfully select patients for limited resection. While the previous study included both primary and metastatic lung cancers [26], metastatic lung cancers were excluded in the present study, in order to compare the usefulness of the two procedures to evaluate the aggressiveness of NSCLC. In addition, while the previous study included tumors larger than 3 cm in size, the present study was targeted at NSCLC measuring less than 3 cm in size to compare the ability of assessing tumor aggressiveness to select patients for limited resection between the DWI and FDG-PET, and because FDG uptake is dependent on the tumor size [32].

Materials and Methods

Eligibility

The examination of both DWI and FDG-PET in patients with lung cancer was approved by the Ethical Committee of Kumamoto University Hospital in January 2006. Informed consent was obtained from all patients after explaining the costs and benefits of the examinations with their surgeons.

Patients

Between February 2006 and December 2007, 144 patients with 182 pulmonary lesions underwent both FDG-PET and DWI, which were done within 2 weeks of each other. Of these lesions, 22 lesions larger than 3 cm in size and 11 metastatic lung cancers were excluded from this study. Twenty-five lesions with the appearance of pure ground-glass opacity (GGO) were also excluded, because all these nodules were negative on both DWI and PET. After these exclusions, 110 patients with a total of 124 nodules were entered in the study (Table 1). There were 56 men and 54 women with a mean age of 68 ± 9 years (range: 36–82 years). Of the 124 nodules, 106 were diagnosed histologically after surgical resection, while 18 were diagnosed as old inflammation because their sizes had been unchanged for more than 2 years upon review of retrospective chest X-ray films or CT. Mean follow-up duration of these 18 nodules, of which 6 were checked by X-ray and the other 12 by CT, was 41±23 months (range: 24-97 months). Mean size of these 18 nodules was 1.6±0.6 cm (range:

1.0-3.0cm). None of the 124 lesions had apparent cavitations and calcifications on CT. Long-axis diameter of pulmonary nodules was selected as size of the lesions.

PET-CT scanning

Patients were instructed to fast for at least 5 hours before intravenous administration of FDG. The dose of FDG administered was 100 μCi/kg (3.7 MBq/kg) of body weight. PET imaging was performed approximately 60 minutes after intravenous administration of FDG using an integrated PET/CT device (Discovery ST; GE Medical Systems) that consisted of a PET scanner (Advance Nx; GE Medical Systems) and an eight-section CT scanner (Light Speed Plus; GE Medical Systems). All images were acquired under shallow-breathing conditions.

The acquisition time for PET in 3D mode was 3 minutes per table position. CT data were resized from a 512 x 512 matrix to a 128 x 128 matrix to match the PET data to allow image fusion, and a CT transmission map was generated. PET image data was reconstructed iteratively using the ordered subsets expectation-maximization algorithm with segmented attenuation correction (4 iterations, 28 subsets) and the CT data. The 3.75 mm thick transaxial CT images were reconstructed at 3.27 mm intervals (transaxial) for fusion with the transaxial PET images. The PET, CT, and fused images were available for review in the axial, coronal, and sagittal planes using a software (Xeleris; GE Medical Systems) on a computer workstation.

Diffusion-weighted imaging (DWI)

All MR images were obtained with a 1.5 T superconducting system (Gyroscan Intera Achieva Nova Dual; Philips Medical Systems, the Netherlands). Conventional MR images and DWI were acquired during the same procedure. The conventional MR images consisted of a coronal T1-weighted sequence (repetition time [TR] msec/ echo time [TE] msec/excitations, 234/4/1), and coronal and axial single shot spin echo T2-weighted (800/90/1), and coronal and axial short tau inversion recovery (STIR)(TR/TE/inversion time, 4600/90/160) sequences. The T1-weighted, T2-weighted, and STIR sequences were acquired at a section thickness of 6 mm with a 1-mm intersection gap, a 128 x 128 matrix, and a 40-45cm field of view (FOV). All images were acquired under shallow-breathing conditions.

DWI was performed in the transverse plane using a spin-echo, echo-planar imaging sequence with the following parameters: TR/TE/flip angle, 5900/60/90; diffusion gradient encoding in 3 orthogonal directions; b=1000 s/mm^2; FOV, 400 mm; matrix size, 112x100; section thickness, 6 mm; section gap, 1 mm; and number of signals acquired, 6.

PET Data Analysis

One radiologist (S.S. with 11 years of radioisotope scintigraphy and PET experience) who was unaware of the patients' clinical data evaluated the PET-CT data. After image reconstruction, a two-dimensional (2D) circular region of interest (ROI) was drawn in a slice after visual detection of the highest count on the fused CT image. For the lesions with negative or faintly positive PET findings, the ROI was drawn on the fusion image with the corresponding CT. From these ROI, the maximum SUV

value (SUV-max) was calculated. The contrast ratio of SUV (SUV-CR) was then calculated as described previously [33,34]. Briefly, the values of SUV-max in the tumor ROI (T) and at the equivalent point in the contralateral normal lung (N) were measured. The SUV-CR was calculated by (T-N)/(T+N) in each lesion as an index of FDG uptake.

DWI Data Analysis

One radiologist (K.K. with 17 years of MRI experience) who was unaware of the patients' clinical data evaluated the MRI image. DWI data were evaluated semiquantitatively using ADC. The ADC was calculated as follows: $ADC = -[\ln(S/S_0)]/b$, where S is the signal intensity (SI) of the ROI obtained through 3 orthogonally oriented DWIs or diffusion trace images, and b is a gradient b factor with a value of 1000 s/mm^2. After image reconstruction, a 2D square ROI was drawn in a slice where the lesion was detected visually with reference to the T2-weighted image or CT. From the ROI, the minimum ADC value was calculated. The mean ADC was not used because the value within the entire tumor might not characterize the tumor owing to its heterogeneity [35].

Determining the cutoff value of ADC and SUV-CR

A receiver operating characteristic (ROC) curve was constructed according to the ADC and SUV-CR using SPSS software (SPSS 15.0 J for Windows, SPSS, Chicago, IL), and the cutoff values were determined for benign/malignant discrimination. Nodules with less than the cutoff value of ADC were defined as

positive on DWI. Nodules with more than the cutoff value of SUV-CR were defined as positive on PET-CT.

Pathological analysis

Hematoxylin and eosin and Elastica-van Gieson staining were performed on all sections to investigate lymphatic, vascular, and pleural involvements. Grade of histological differentiation in adenocarcinoma was classified into well-differentiated (W/D), moderately-differentiated (M/D), and poorly-differentiated (P/D). Pleural involvement was classified as p0, p1, p2, and p3; that is, a p0 tumor did not extend beyond the pleural elastic layer, a p1 tumor invaded the visceral pleural elastic layer, but did not reach the pleural surface, a p2 tumor included tumor exposure on the pleural surface, and a p3 tumor invaded the parietal pleura or the chest wall. Pathological tumor stages were based on the TNM classification of the International Union Against Cancer [36]: p2 tumors were classified as T2, p3 tumors were classified as T3, and tumors with intrapulmonary metastases within the same lobe were classified as T4.

Analysis of the tumor aggressiveness

The aggressiveness of NSCLC was evaluated based on the pathological tumor stage, the tumor invasiveness as determined by lymphatic, vascular and/or pleural involvements, and the grade of histological differentiation and the Ki-67 staining score of the adenocarcinoma, because these factors are known to be related to the patients' prognosis [3,37,38]. To evaluate the usefulness of DWI and PET to predict

the tumor aggressiveness, the values of ADC and the SUV-CR were compared between pathological stage IA and IB or more advanced stage, between tumors with and without lymphatic, vascular and/or pleural involvement, between W/D and M/D or P/D adenocarcinomas and baced on proliferative activity determined by Ki-67 staining score.

Evaluation of immunohistochemical staining with Ki-67

To examine the proliferative activity of adenocarcinoma, immunostaining with Ki-67 was performed by using the Dako envision system (Dako Cytomation, Glostrup, Denmark). Antibody for Ki-67 (monoclonal mouse antibody MIB-1) was purchased from Dako Co. Sections of 4 μm were cut from the paraffin blocks. Immunostaining was performed with antigen-retrieval techniques as previously described [31]. According to the method of Martin et al. [39], the Ki-67 staining score was measured by determining the percentage of cells with positive nuclei in more than 1000 tumor cells in more than 4 fields.

Statistical analysis

The differences of sensitivity and specificity between DWI and PET were analyzed using the McNemar test. True-positive (TP), true-negative (TN), false-positive (FP), and false-negative (FN) results of PET-CT and DWI images for detecting pulmonary malignancies were compared with the results of pathological diagnosis or follow-up examination. Sensitivity was calculated as TP/TP+FN,

specificity as TN/TN+FP, and accuracy as TP+TN/total. Positive predictive value and negative predictive value were calculated as TP/TP+FP and TN/TN+FN, respectively, and the difference of them between DWI and PET were analyzed by Student's t-test. Student's t-test was also used to compare the distribution of size between malignant and benign nodules, the values of ADC and SUV-CR at pathological stage IA and IB or more advanced stages, and these values in tumors which were or were not invasive. The correlations among ADC-min, SUV-CR and Ki-67 staining score were analyzed using Pearson's r-test. Statistical analysis was performed using SPSS software. All values in the text and tables are given as mean ± standard deviation. A difference with a P value of less than 0.05 was considered as significant for all analyses.

Results

Histological type of NSCLC was adenocarcinoma in 76 lesions, squamous cell carcinoma in 17, and adenosquamous carcinoma in 3. The grade of histological differentiation in adenocarcinoma was W/D in 57 lesions, M/D in 14, and P/D in 5. Pathological stage was IA in 75 lesions and IB or more advanced stages in 21 (Table 1). Benign nodules showed acute inflammation in 4 lesions, chronic inflammation in 20, hamartoma in 2, and other lesions in 2. There was no significant difference in mean size of NSCLC and benign lesions.

DWI clearly identified the malignant nodules in a fashion similar to PET imaging (Fig. 1). The ROC curves for the benign/malignant discrimination showed the optimal cutoff values of ADC on DWI to be 1.2×10^{-3} mm^2/s and SUV-CR on PET to be 0.31 on PET (Fig.2a,b).

In the 96 NSCLC nodules, DWI was positive in 70 and negative in 26, while PET was positive in 69 and negative in 27 (Table 2). Of the 57 W/D adenocarcinomas, 24 (42%) and 25 (44%) were negative on DWI and PET, respectively. None of the 5 P/D adenocarcinomas, l7 squamous cell carcinomas and 3 adenosquamous carcinomas was negative with DWI or PET. In the 28 benign nodules, DWI was positive in one and negative in 27, while PET was positive in 5 and negative in 23 (Table 3).

Tables 4 and 5 shows the results achieved using the McNemar test. Table 4 shows the correlation between DWI and PET in diagnosis of NSCLC. There was no

significant difference of sensitivity between DWI and PET (p=1.0). Table 5 shows the correlation between DWI and PET in diagnosis of benign nodules. There was no significant difference of specificity between DWI and PET (p=0.22). The accuracy of DWI and PET were 0.78 and 0.74, respectively, which showed no significant difference (p= 0.69). Positive predictive values of DWI and PET were 0.98 and 0.93, respectively, of which difference was not significant (p=0.83). Negative predictive values of DWI and PET were 0.51 and 0.46, respectively, of which difference was not significant (p=0.31).

Table 6 showed the mean values of ADC in DWI and SUV-CR in PET with their relationship to the pathological tumor stage, tumor invasiveness of NSCLC, and grade of histological differentiation in adenocarcinoma. While DWI did not show the significant difference of the mean value of ADC in these subgroups, PET showed a significant difference in SUV-CR between NSCLC at pathological stage IA and IB or more advanced stages, between NSCLC with and without lymphatic, vascular, and pleural involvements, and between W/D and M/D or P/D adenocarcinomas ($p<0.01$ – 0.001).

While SUV-CR and Ki-67 staining scores showed a significant correlation with each other ($r=0.410$, $p<0.001$) (Fig. 3b), ADC did not correlate with Ki-67 staining scores ($r=-0.125$, $p=0.31$) (Fig. 3a).

Discussion

The present study showed that sensitivity and specificity of DWI and PET for differentiating between NSCLC and benign pulmonary nodules were not different. We therefore conclude that DWI can be used in place of PET for discrimination between benign and NSCLC.

On the other hand, DWI could not predict the aggressiveness of NSCLC or adenocarcinoma as well as PET. It has been reported that FDG-PET can predict the aggressiveness of NSCLC [28-31], because tumors with low aggressiveness have low rate of glucose-metabolism. We previously reported that the FDG uptake could be used to predict the aggressiveness of lung adenocarcinoma, i.e. lung adenocarcinomas with high FDG uptake had more frequent lymph node metastasis, higher tumor invasiveness, higher proliferative activity, and poorer prognosis than those with low FDG uptake [29-31]. Because the ADC value in DWI of tumors is known to decrease with increased cellularity, larger nuclei, and larger N/C ratio [17,18], we initially hypothesized that the ADC value might correlate with the aggressiveness of NSCLC as well as FDG uptake in PET. In brain glioma and astrocytoma, Murakami et al. reported that ADC values showed a significant correlation with the histological grade of malignancy and prognosis [18], supporting our hypothesis. However, the present study demonstrated that ADC in DWI did not show a significant correlation with pathological tumor stage and tumor invasiveness of NSCLC and the grade of histological differentiation of adenocarcinoma, while FDG uptake in PET did. We therefore conclude that while DWI can image NSCLC as well as PET, it cannot

predict the tumor aggressiveness of NSCLC or adenocarcinoma.

The following reasons might explain why ADC values in NSCLC did not correlate with the tumor aggressiveness, differing from the results in brain glioma and astrocytoma [18]: (1) The difference in magnetic susceptibility at the tumor-lung interface creates inhomogeneity in the local magnetic field which disrupts the MR signals of lung tumors, like the artifacts which arise from the heart-lung interface [40]; and (2) Respiratory and cardiac motion causes additional image artifacts and signal loss [41].

One of the deficiencies of FDG-PET in diagnosis of lung cancer is its FN results for W/D adenocarcinoma, which is due to their low rate of glucose-metabolism and low density [32]. The present study showed that both DWI and PET were negative in approximately 40% of W/D adenocarcinoma, suggesting that DWI does not compensate for the PET deficiency in this regard. We therefore hold the opinion that W/D adenocarcinomas are difficult to diagnose using either PET or DWI.

Although SUV has been used frequently for evaluation of FDG-PET, it is well known that several factors can affect the SUV, such as body size [42] and blood glucose level [43]. We previously compared the results of SUV-max, SUV-CR with contralateral lung, and SUV-CR with cerebellum for pulmonary nodules, and reported that SUV-CR with contralateral lung or cerebellum showed significantly higher sensitivity than SUV-max [33], a conclusion which was supported by Obrzut [44]. Therefore, we selected SUV-CR with contralateral lung for analysis in this study.

While FDG-PET is useful for imaging the whole body, DWI does not have

that ability, because of the need for breath holding by the patient during the imaging. Recently, Takahara et al. developed a new technology of DWI that can be conducted under normal breathing, and allows acquisition of more slices with multiple signal averaging, higher signal-to-noise ratio, and high-quality maximum-intensity projection images [16], enabling whole-body imaging [24]. Ohno et al. recently reported that the whole-body MRI with DWI showed similar sensitivity for M-staging to PET/CT [27]. We also reported that DWI can be used in place of PET-CT for N-staging of NSCLC [45]. However, ADC values in DWI are known to be different among MR machines. Therefore, as the next step, a multicenter study should be conducted to determine whether or not whole-body DWI can be used for imaging of the systemic metastasis in lung cancer like FDG-PET.

Currently, small peripheral NSCLC is being increasingly seen, due to the development of diagnostic devices such as high-resolution computed tomography [1]. If complete resection of tumor cells is possible with limited resections such as wedge resection, segmentectomy and omission of lymphadenectomy, these techniques may become the standard procedures for small peripheral NSCLC. Furthermore, the development of video-assisted surgery has permitted minimal invasiveness in general thoracic surgery and has benefited high risk patients [2─6]. Thus, a proportion of patients with small peripheral NSCLC may be cured using limited resection involving these less invasive procedures. Having said that, the choice of surgical procedure for such patients remains controversial. Strong evidence for lobectomy for stage I NSCLC as the procedure of choice, compared with limited resection, has arisen from

randomized controlled trials performed by the Lung Cancer Study Group [46]. They indicated that patients who underwent limited resection, such as wedge resection and segmentectomy, had an increased risk of local recurrence and reduced survival. To successfully select patients for limited resection, patients with good prognosis preoperatively should be chosen. The present study showed that DWI can be used in place of PET for imaging NSCLC. However, it should be kept in mind that DWI cannot predict the aggressiveness of NSCLC as well as FDG-PET does.

Conclusions

The present study showed that DWI is equivalent to FDG-PET in distinguishing non–small cell lung cancer from benign pulmonary nodules but is not as useful for predicting aggressiveness of non–small cell lung cancer.

Clinically defined peripheral stage IA NSCLC should be carefully considered for a limited operations when high SUV-CR value are observed.

References

1. Rusch VW. High-resolution computed tomography in clinical T1 N0 M0 adenocarcinoma of the lung. J Thorac Cardiovasc Surg 2002;124:221-2.

2. Demmy TL, Curtis JJ. Minimally invasive lobectomy directed toward frail and high-risk patients: a case-control study. Ann Thorac Surg 1999;68:194-200.

3. Shennib H, Bogart J, Herndon JE, Kohman L, Keenan R, Green M, et al. Video-assisted wedge resection and local radiotherapy for peripheral lung cancer in high-risk patients: the Cancer and Leukemia Group B (CALGB) 9335, a phase II, multiinstitutional cooperative group study. J Thorac Cardiovasc Surg 2005;129:813-8.

4. Santambrogio L, Nosotti M, Bellaviti N, Mezzetti M. Videothoracoscopy versus thoracotomy for the diagnosis of the indeterminate solitary pulmonary nodule. Ann Thorac Surg 1995;59:868-70.

5. Roviaro G, Varoli F, Vergani C, Maciocco M, Nucca O, Pagano C. Video-assisted thoracoscopic major pulmonary resections: technical aspects, personal series of 259 patients, and review of the literature, Part 2. Surg Endosc 2004.

6. DeCamp Jr MM, Jaklitsch MT, Mentzer SJ, Harpole Jr DH, Sugarbaker DJ. The safety and versatility of video-thoracoscopy: a prospective analysis of 895 consecutive cases. J Am Coll Surg 1995;181:113-20.

7. Nakamura H, Kawasaki N, Taguchi M, Kabasawa K. Survival following lobectomy vs limited resection for stage I lung cancer: a meta-analysis. Br J

Cancer 2005;92:1033-7.

8. Watanabe T, Okada A, Imakiire T, Koike T, Hirono T. Intentional limited resection for small peripheral lung cancer based on intraoperative pathologic exploration. Jpn J Thorac Cardiovasc Surg 2005;53:29-35.

9. Kawahara K, Iwasaki A, Yoshinaga Y, Shiraishi T, Okabayashi K, Tohchika H, et al. Lymph node metastasis and prognosis in small peripheral non-small-cell lung cancers. Jpn J Thorac Cardiovasc Surg 2000;48:618-24.

10. Ohta Y, Oda M, Wu J, Tsunezuka Y, Hiroshi M, Nonomura A, et al. Can tumor size be a guide for limited surgical intervention in patients with peripheral non-small cell lung cancer? Assessment from the point of view of nodal micrometastasis. J Thorac Cardiovasc Surg 2001;122:900-6.

11. Takizawa T, Terashima M, Koike T, Watanabe T, Kurita Y, Yokoyama A, et al. Lymph node metastasis in small peripheral adenocarcinoma of the lung. J Thorac Cardiovasc Surg 1998;116:276-80.

12. Suzuki K, Asamura H, Kusumoto M, Kondo H, Tsuchiya R. Early peripheral lung cancer: prognostic significance of ground glass opacity on thin-section computed tomographic scan. Ann Thorac Surg. 2002; 74:1635-9.

13. Matsuguma H, Yokoi K, Anraku M, et al. Proportion of ground-glass opacity on high-resolution computed tomography in clinical T1 N0 M0 adenocarcinoma of the lung: a predictor of lymph node metastasis. J Thorac Cardiovasc Surg. 2002;124:278-84.

14. Wang J, Takashima S, Takayama F, Kawakami S, Saito A, Matsushita T, et al. Head and Neck lesions: characterization with diffusion-weighted echo-planar MR imaging. Radiology 2001; 220: 621-30.

15. Sumi M, Takagi Y, Uetani M, Morikawa M, Hayashi K, Kabasawa H, et al. Diffusion-weighted echoplanar MR imaging of salivary glands. AJR 2002; 178: 959-65.

16. Takahara T, Imai Y, Yamashita T, Yasuda S, Nasu S, Van Cauteren M. Diffusion weighted whole body imaging with background body signal suppression (DWIBS): Technical improvement using free breathing, STIR and High Resolution 3D Display. Rad Med 2004; 22: 275-82.

17. Nasu K, Kuroki Y, Kuroki S, Murakami K, Nawano S, Moriyama N. Diffusion-weighted Single Shot Echo Planar Imaging of Colorectal Cancer Using a Sensitivity-encoding Technique. Jpn J Clin Oncol 2004; 34: 620-26.

18. Murakami R, Sugahara T, Nakamura H, Hirai T, Kitajima M, Hayashida Y, et al. Malignant supratentorial astrocytoma treated with postoperative radiation therapy: prognostic value of pretreatment quantitative diffusion-weighted MR imaging. Radiology 2007; 243:493-9.

19. Woodhams R, Matsunaga K, Kan S, Hata H, Ozaki M, Iwabuchi K, et al. ADC Mapping of Benign and Malignant Breast Tumors. Magn Reson Med Sci 2005; 4: 35-42.

20. Hayashida Y, Yakushiji T, Awai K, Katahira K, Nakayama Y, Shimomura O, et al. Monitoring therapeutic responses of primary bone tumors by diffusion-weighted image: initial results. Eur Radiol 2006; 16: 2637-43.

21. Reinsberg SA, Payne GS, Riches SF, Ashley S, Brewster JM, Morgan VA, et al. Combined use of Diffusion-Weighted MRI and 1H MR Spectroscopy to Increase Accuracy in Prostate Cancer Detection. AJR 2007; 188: 91-98.

22. Dzik-Jurasz A, Domenig C, George M, Wolber J, Padhani A, Brown G, et al. Diffusion MRI for prediction of response of rectal cancer to chemoradiation. Lancet 2002; 360: 307-08.

23. Matoba M, Tonami H, Kondou T, Yokota H, Higashi K, Toga H, et al. Lung Carcinoma: Diffusion weighted MR Imaging—Preliminary Evaluation with Apparent Diffusion Coefficient. Radiology 2007; 243:570-7.

24. Komori T, Narabayashi I, Matsumura K, Matsuki M, Akagi H, Ogura Y, et al. 2-[Fluorine-18]-fluoro-2-deoxy-D-glucose positron emission tomography/computed tomography versus whole-body diffusion-weighted MRI for detection of malignant lesions: initial experience. Ann Nucl Med 2007; 21:209-15.

25. Lichy MP, Aschoff P, Plathow C, Stemmer A, Horger W, Mueller-Horvat C, et al. Tumor detection by diffusion-weighted MRI and ADC-mapping. Initial clinical experiences in comparison to PET-CT. Invest Radiol 2007; 42:605-13.

26. Mori T, Nomori H, Ikeda K, et al. Diffusion-weighted magnetic resonance imaging for diagnosing malignant pulmonary nodules/masses. J Thorac Oncol 2008; 3:358-64.

27. Ohno Y, Koyama H, Onishi Y, et al. Non-small cell lung cancer : whole-body MR examination for M-stage assessment – Utility for whole-body diffusion-weighted imaging compared with integrated FDG PET/CT. Radiology 2008; 248:643-654.

28. Cerfolio RJ, Bryant AS, Ohja B, Bartolucci AA. The maximum standardized uptake values on positron emission tomography of a non-small cell lung cancer

predict stage, recurrence, and survival. J Thorac Cardiovasc Surg 2005;130:151-159

29. Nomori H, Watanabe K, Ohtsuka T, Naruke T, Suemasu K, Kobayashi T, et al. Fluorine 18 –tagged fluorodeoxyglucose positron emission tomographic scanning to predict lymph node metastasis, invasiveness, or both, in clinical T1 N0 M0 lung adenocarcinoma. J Thorac Cardiovasc Surg 2004; 128: 396-401.

30. Ohtsuka T, Nomori H, Watanabe K, Kaji M, Naruke T, Suemasu K, et al. Prognostic significance of [18F] fluorodeoxyglucose uptake on positron emission tomography in patients with pathologic stage I lung adenocarcinoma. Cancer 2006; 107:2468-73.

31. Watanabe K, Nomori H, Ohtsuka T, Naruke T, Ebihara A, Orikasa H, et al. [F-18] Fluorodeoxyglucose positron emission tomography can predict pathological tumor stage and proliferative activity determined by Ki-67 in clinical stage IA lung adenocarcinomas. Jpn J Clin Oncol 2006;36:403-409.

32. Menda Y, Bushnell DL, Madsen MT, McLaughlin K, Kahn D, Kernstine KH. Evaluation of various corrections to the standardized uptake value for diagnosis of pulmonary malignancy. Nucl Med Commun 2001;22:1077–81.

33. Nomori H, Watanabe K, Ohtsuka T, Naruke T, Suemasu K, Uno K. Evaluation of F-18 fluorodeoxyglucose (FDG) PET scanning for pulmonary nodules less than 3cm in diameter, with special reference to CT images. Lung Cancer 2004; 45:19-27.

34. Nomori H, Watanabe K, Ohtsuka T, Naruke T, Suemasu K, Uno K. Visual and semiquantitative analyses for F-18 Fluorodeoxyglucose PET scanning in pulmonary nodules 1cm to 3cm in size. Ann Thorac Surg 2005;79:984-88

35. Koh DM, Padhani AR. Diffusion-weighted MRI: a new functional clinical technique for tumor imaging. Br J Radiol 2006; 79:633-5.

36. Sobin LW, Witteking CH. UICC TMN classification of malignant tumors. 6th Ed. New York: Wiley-Liss 2002;131-41.

37. Brechot JM, Chevret S, Charpentier MC, et al. Blood vessel and lymphatic vessel invasion in resected non-small cell lung carcinoma. Cancer 1996; 78:2111-8.

38. Takise A, Kodama T, Shimosato Y, Watanabe S, Suemasu K. Histopathologic prognostic factors in adenocarcinomas of the peripheral lung less than 2 cm in diameter. Cancer. 1988 61:2083-8.

39. Martin B, Paesmans M, Mascaux C, Berghmans T, Lothaire P, MeertA, et al. Ki-67 expression and patients survival in lung cancer: systematic review of the literature with meta-analysis. Br J Cancer 2004;91:2018-25

40. Atalay MK, Poncelet BP, Kantor HL, Brady TJ, Weisskoff RM. Cardiac susceptibility artifacts arising from the heart-lung interface. Magn Reson Med 2001; 45:341-345.

41. Chen BT, Yordanov AT, Johnson GA. Ventilation-synchronous magnetic resonance microscopy of pulmonary structure and ventilation in mice. Magn Reson Med. 2005; 53:69-75.

42. Kim CK, Gupta NC, Chandramouli B, Alavi A. Standardized uptake values of FDG: body surface area correction is preferable to body weight correction. J Nucl

Med 1994;35:164-7.

43. Lindholm P, Minn H, Leskinen-Kallio S, Bergman J, Ruotsalainen U, Joensuu H. Influence of the blood glucose concentration on FDG uptake in cancer-a PET study. J Nucl Med 1993;34:1-6

44. Obrzut S, Pham RH, Vera DR, Badran K, Hoha CK. Comparison of lesion-to-cerebellum uptake ratios and standardized uptake values in the evaluation of lung nodules with 18F-FDG PET. Nuclear Medicine 2007; 27:7-13.

45. Nomori H, Mori T, Ikeda K, et al. Diffusion-Weighted Magnetic Resonance Imaging for N-Staging of Lung Cancer: Comparison with Positron Emission Tomography. J Thorac Cardiovasc Surg. 2008; 135:816-822.

46. Ginsberg RJ, Rubinstein LV. Randomized trial of lobectomy versus limited resection for T1 N0 non-small cell lung cancer. Lung Cancer Study Group. Ann Thorac Surg 1995;60:615—22.

Figures and tables

Figure 1. Lung adenocarcinoma in the right lower lobe. (a) Computed tomography, (b) diffusion weighted image, and (c) fluorodeoxyglucose-positron emission tomography. Arrows indicate the tumor images on DWI and PET. The minimum value of the apparent diffusion coefficient, the maximum standard uptake value, and the contrast ratio of standard uptake value in the tumor are 0.98 $x10^{-3}$ mm^2/s, 3.2, and 0.68, respectively.

Figure 2. (a) The receiver operating characteristic curve of the minimum value of the apparent diffusion coefficient for diagnosing non-small cell lung cancer in pulmonary nodules, showing the optimal cutoff value to be $1.2x10^{-3}$ mm^2/s (indicated by an arrow). Area under curve: 0.91 (95% confidence interval: 0.86 – 0.97).
ADC: minimum value of apparent diffusion coefficient.

Figure 2. (b) The receiver operating characteristic curve of the contrast ratio of the standard uptake value for diagnosing non-small cell lung cancer, showing the optimal cutoff value to be 0.31 (indicated by an arrow). Area under curve:0.82 (95% confidence interval: 0.75 – 0.90). SUV-CR: contrast ratio of standard uptake value.

Figure 3. (a) Correlation plots between ADC-min and Ki-67 staining scores. (b) Correlation plots between SUV-CR and Ki-67 staining scores. The solid line shows

the linear regression line and the broken lines show the 95% confidence interval. SUV-CR: contrast ratio of standard uptake value; ADC-min: minimum apparent diffusion coefficient.

Figure 1a

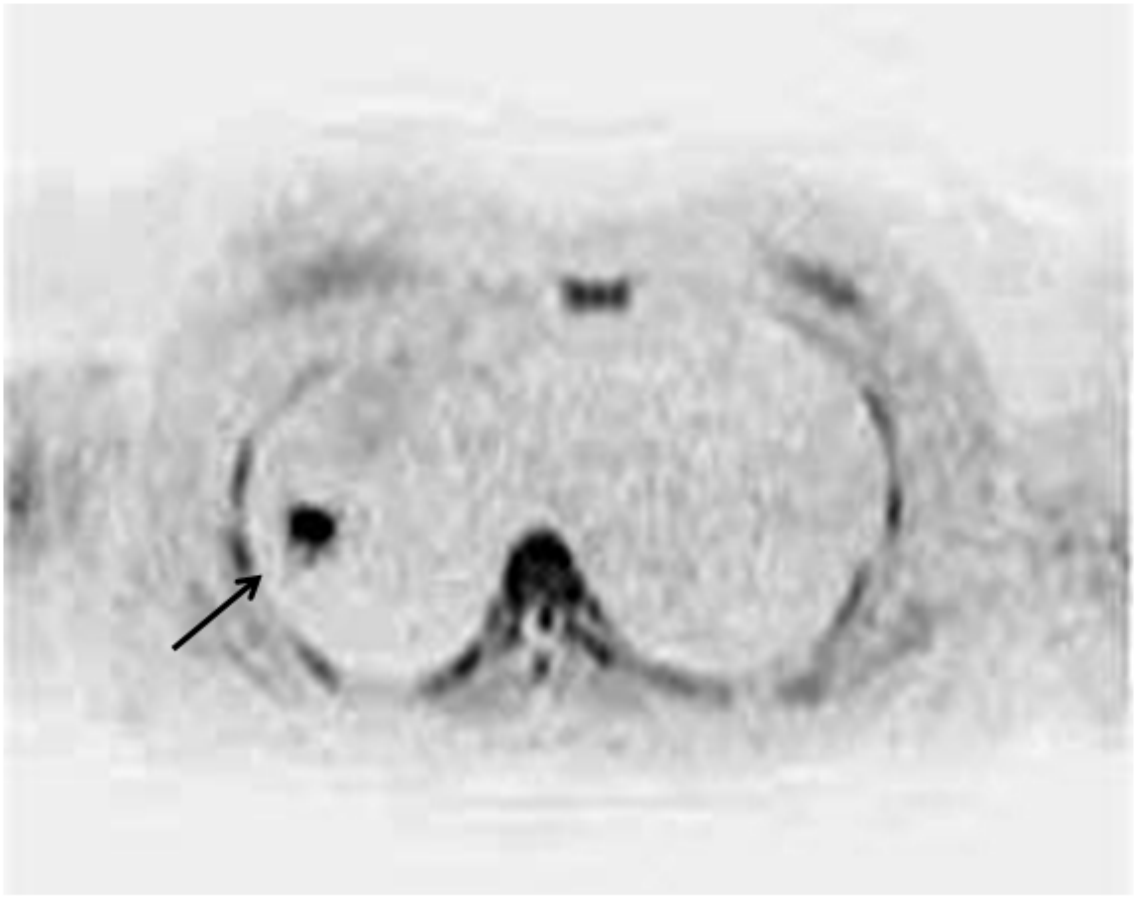

Figure 1b

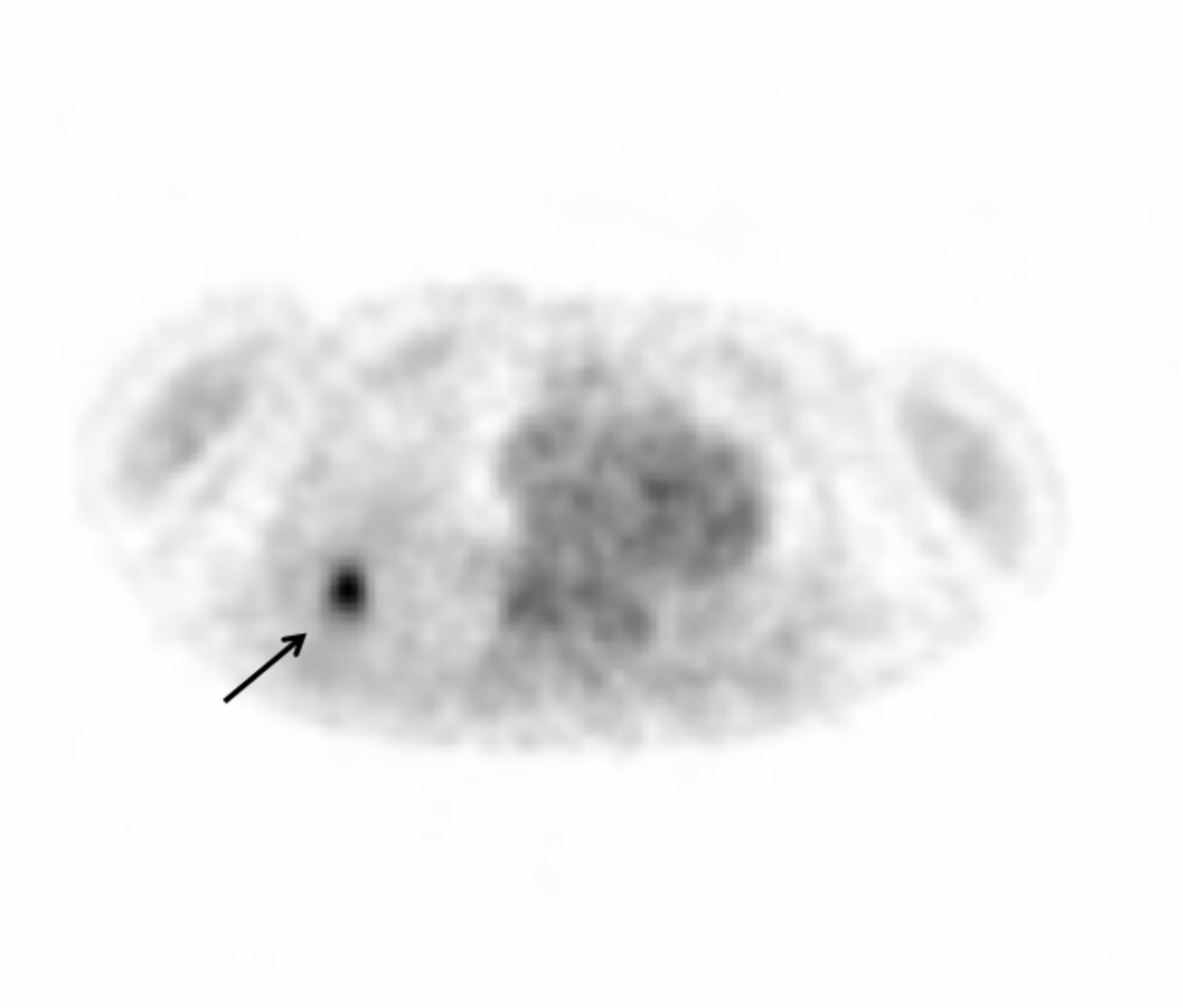

Figure 1c

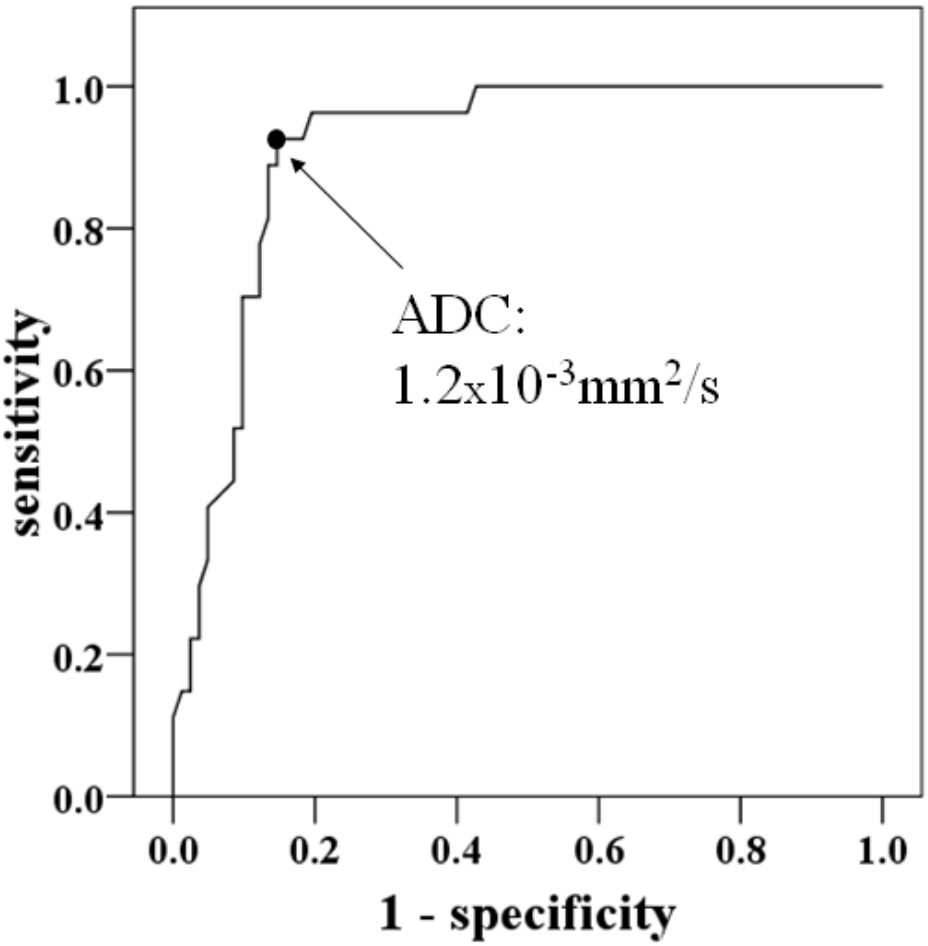
1.0
0.8
0.6
0.4
0.2
0.0
sensitivity
ADC:
1.2x10-3mm2/s
0.0
0.2
0.4
0.6
0.8
1.0
1 - specificity

Figure 2a

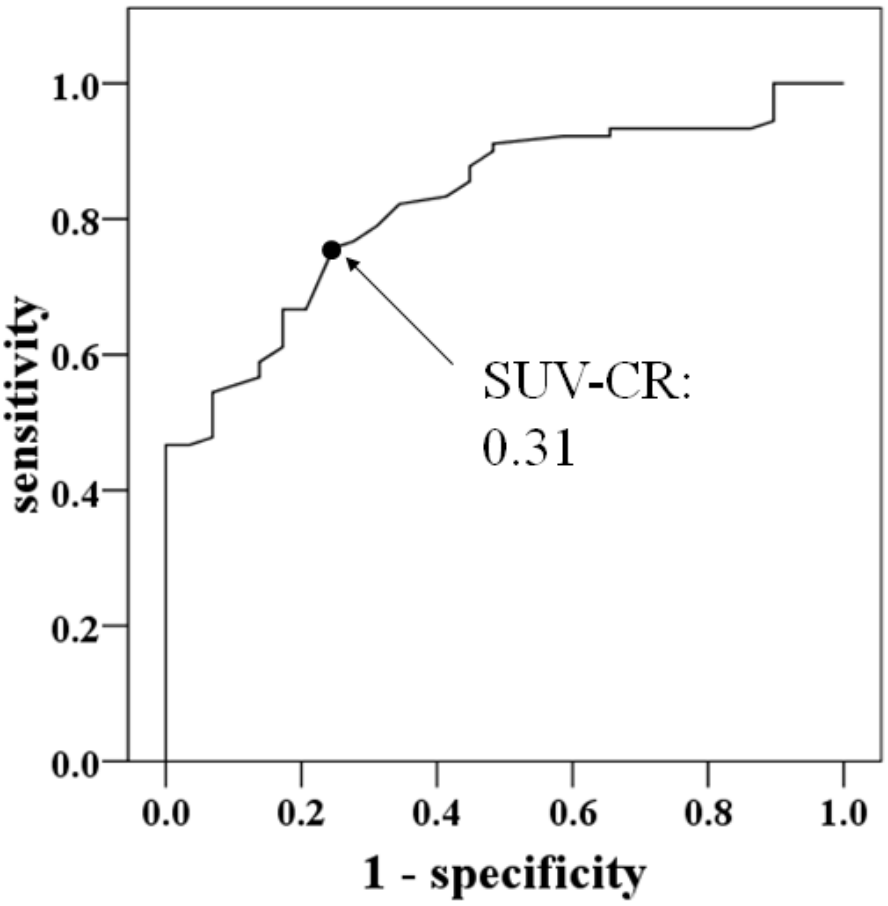
1.0
0.8
0.6
0.4
0.2
0.0
sensitivity
SUV-CR:
0.31
0.0
0.2
0.4
0.6
0.8
1.0
1 - specificity

Figure 2b

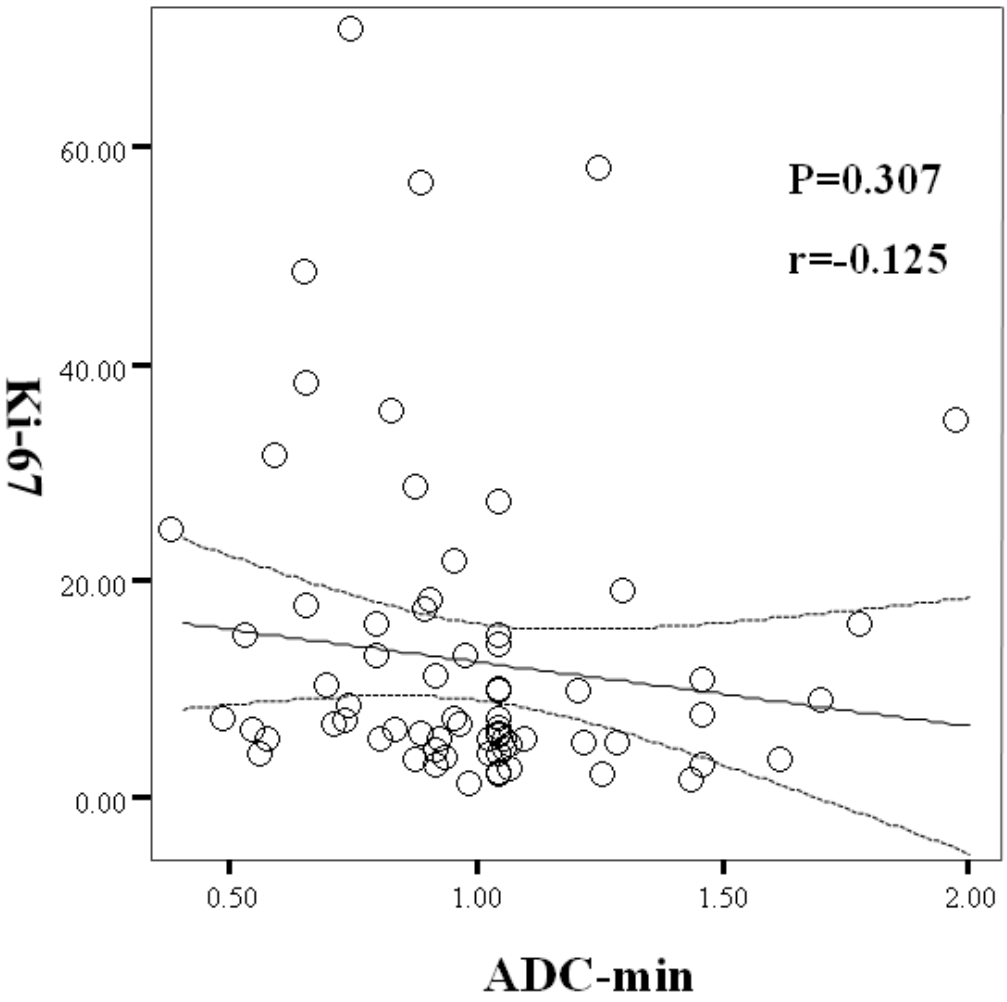

Figure 3a

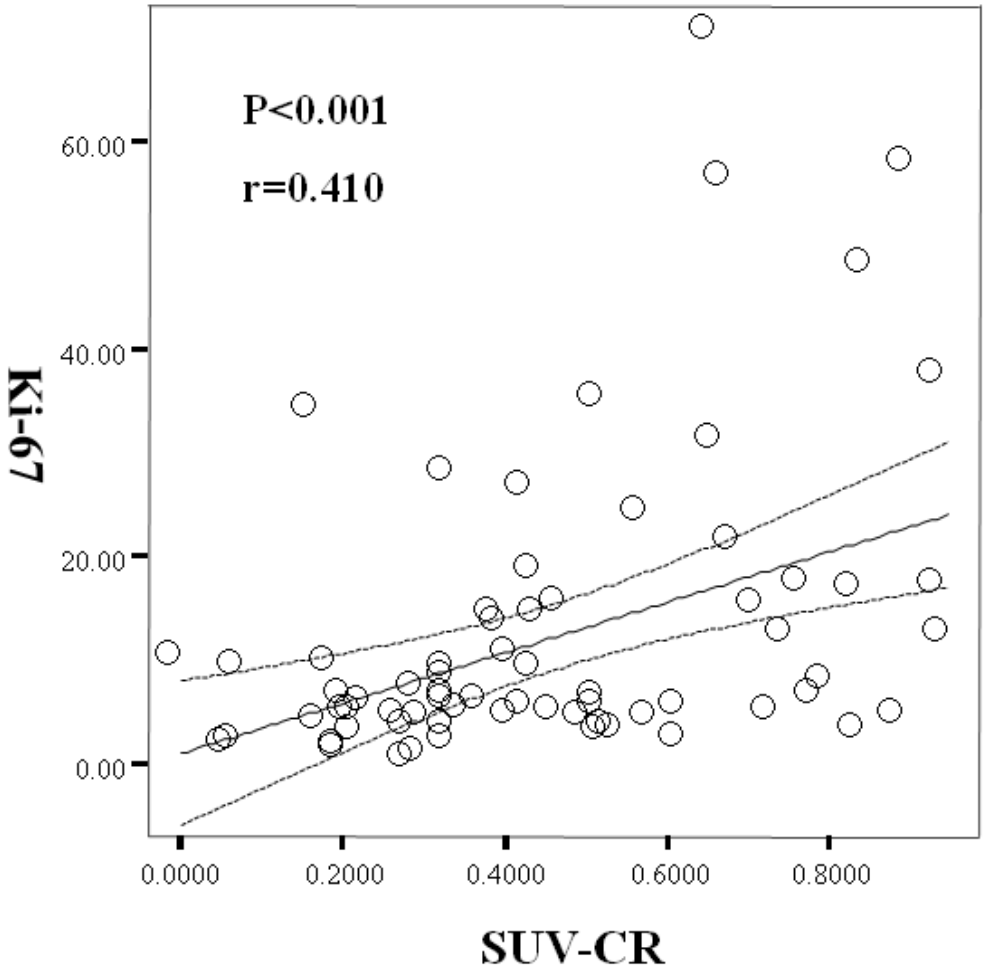
P<0.001
r=0.410
60.00
40.00
20.00
0.00
Ki-67
0.0000
0.2000
0.4000
0.6000
0.8000
SUV-CR

Figure 3b

Table 1 Characteristics of non-small cell lung cancer and benign nodules

Non-small cell lung cancer (n=96)		
Mean size (cm)(range)	1.6 ± 0.7 (1.0－3.0)	
Histological type		
Adenocarcinoma	76	
Well-differentiated		57
Moderately-differentiated		14
Poorly-differentiated		5
Squamous cell carcinoma	17	
AdenoSquamous carcinoma	3	
Pathological stage		
IA	75	
IB−IV	21	
T1N1M0		5
T3N0M0		2
T3N1M0		3
T1N2M0		4
T3N2M0		3
T4N2M0		3
T1N1M1		1
Benign nodules (n=28)		
Mean size (cm) (range)	1.5 ± 0.7 (1.0－3.0)	
Type		
Acute inflammation	4	
Chronic inflammation	20	
Hamartoma	2	
Others	2	

Table 2. Findings of diffusion-weighted imaging and positron emission tomography in non-small cell lung cancer

	DWI		PET		
Histology	Positive	Negative	Positive	Negative	Total
Adenocarcinoma					
Well-differentiated	33	24	32	25	57
Moderately-differentiated	12	2	12	2	14
Poorly-differentiated	5	0	5	0	5
Squamous cell carcinoma	17	0	17	0	17
Adenosquamous carcinoma	3	0	3	0	3
Total	70	26	69	27	96

DWI: diffusion weighted imaging; PET: positron emission tomography

Table 3 Findings of diffusion-weighted imaging and positron emission tomography in benign pulmonary nodules

	DWI		PET		
Histology	Positive	Negative	Positive	Negative	Total
Inflammation					
Acute	1	3	4	0	4
Chronic	0	20	0	20	20
Hamartoma	0	2	0	2	2
Others	0	2	1	1	2
Total	1	27	5	23	28

DWI: diffusion weighted imaging; PET: positron emission tomography

Table 4. Correlation between diffusion-weighted imaging and positron emission tomography for diagnosing non-small cell lung cancer

	PET		
DWI	True-positive	False-negative	Total
True-positive	61	9	70
False-negative	8	18	26
Total	69	27	96

DWI: diffusion weighted imaging; PET: positron emission tomography
Sensitivity of DWI: 0.73(95% Confidence Interval:0.64-0.82)
Sensitivity of PET: 0.72 (95% Confidence Interval:0.63-0.81)
McNemar test: p>.999

Table 5. Correlation between diffusion-weighted imaging and positron emission tomography for diagnosing benign pulmonary nodules

	PET		
DWI	True-negative	False-positive	Total
True-negative	23	4	27
False-positive	0	1	1
Total	23	5	28

DWI: diffusion weighted imaging; PET: positron emission tomography
Specificity of DWI: 0.96(95% Confidence interval:0.90-1.03)
Specificity of PET: 0.82(95% Confidence interval:0.68-0.96)
McNemar test: p=0.22

Table 6. Correlation between the tumor aggressiveness and the values of ADC and SUV-CR

		DWI		PET	
Tumor aggressiveness	Number oftumors	ADC	Difference	SUV-CR	Difference
Tumor stage					
IA	75	1.00±0.34	p=0.08	0.45±0.27	p<0.001
IB-IV	21	0.83±0.20		0.74±0.16	
Lymphatic invasion (-)	79	0.98±0.34	p=0.12	0.46±0.27	p<0.01
(+)	17	0.77±0.18		0.75±0.15	
Vascular invasion (-)	74	0.99±0.37	p=0.08	0.41±0.26	p<0.001
(+)	22	0.85±0.16		0.78±0.14	
Pleural involvement (-)	80	0.97±0.35	p=0.42	0.44±0.27	p<0.001
(+)	16	0.84±0.16		0.78±0.14	
Grade of histological differentiation in adenocarcinoma (n=76)					
W/D	57	1.04±0.37	p=0.11	0.38±0.24	p<0.001
M/D or P/D	19	0.89±0.22		0.61±0.25	

DWI: diffusion weighted imaging; PET: positron emission tomography
ADC: minimum value of apparent diffusion coefficient; SUV-CR: contrast ratio of standard uptake value.
W/D: well-differentiated; M/D: moderately-differentiated; P/D: poorly-differentiated